DESIGN AND ANALYSIS OF A MEMBRANE SUPPORTED FOLDED SLOT ANTENNA FOR W-BAND APPLICATIONS

Alina-Cristina BUNEA[1], Dan NECULOIU[2], Andrei AVRAM[3]

In this paper, we present the first in depth 3D electromagnetic study, design, fabrication and characterization of a W-band (75-110 GHz) membrane supported folded slot antenna. Full-wave 3D electromagnetic simulations are performed for various geometries and field distributions, and scattering (S) parameters, as well as radiation characteristics are analyzed for optimum antenna operation. The fabricated antenna structure has a total membrane area of 3.4 x 1.95 mm^2, showing a measured input matching bandwidth (|S11|< - 10 dB) between 76.3 – 110 GHz. The simulated gain is higher than 4 dBi, with a radiation efficiency higher than 80 % in the whole W-band. These performances make it a good candidate for integration in modern millimeter wave wireless systems.

Keywords: 3D electromagnetic analysis, folded slot antennas, millimeter waves

1. Introduction

Antennas are key components in any wireless communication system, since they provide the link between free space and guided wave propagation. It is essential to have a good understanding of the antenna behavior, even before fabrication, especially since the characterization of antennas can be a difficult task once they are integrated in a system. In millimeter wave applications antennas have to offer not just good functional performances, but also low profile for easy integration with the highly integrated active components, fabricated using silicon and gallium arsenide substrates [1]. But these high-permittivity substrates determine high losses because of dielectric losses and the propagation of substrate modes. The local removing of the substrate underneath the antenna and supporting it on a thin dielectric substrate was the solution proposed in [2] for the first time, for a double dipole antenna.

The semiconductor micromachining technologies have been used for the fabrication of millimeter wave circuits on very thin dielectric membranes, mostly for silicon substrates [3]-[5]. Thin membranes of high quality dielectric materials

[1] PhD Student, University POLITEHNICA of Bucharest, Romania; Research Scientist, National Institute of R&D in Microtechnologies, IMT-Bucharest

[2] Professor, University POLITEHNICA of Bucharest, Romania; Senior Scientist, National Institute of R&D in Microtechnologies, IMT-Bucharest

[3] Research Scientist, National Institute of R&D in Microtechnologies, IMT-Bucharest Corresponding authors: A.C. Bunea: alina.bunea@imt.ro; D.Neculoiu: dan.neculoiu@imt.ro

offer a way of hybrid integration of high quality transmission line structures, filters, antennas and other passive circuits with active components on high resistivity (HR) silicon substrates [6]-[8]. For example, the schematic of a coplanar waveguide (CPW) suspended on a dielectric membrane released through deep reactive ion etching (DRIE) is shown in Fig. 1.

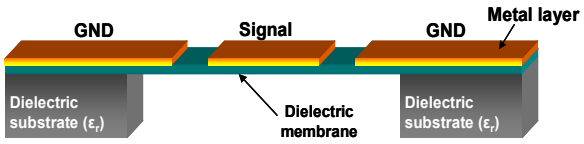

Fig. 1. Schematic of a coplanar waveguide (CPW) suspended on a dielectric membrane

The topology of the folded slot antenna (Fig. 2) designed on semi-infinite substrate was reported in [9]. Structures with single and double folded slots are investigated using analytical approaches for different substrates. These analyses showed that an air supported single folded slot antenna has a fractional matching bandwidth of ~10 %.

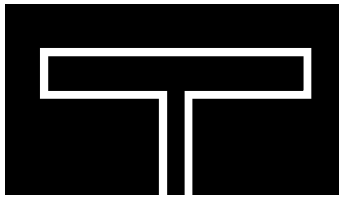

Fig. 2. General layout of a single folded slot antenna

An antenna structure with two folded slots, processed on a two-layer 1.4 μm thick membrane, released through wet micromachining of silicon, was first reported in [5]. The 77 GHz and 94 GHz antennas presented in the paper have an input matching fractional bandwidth of 7 – 8 %, with a simulated gain of 5 – 6 dBi.

For quite a long time an accurate design of the micromachined antenna was limited by the lack of adequate simulation software. To obtain an accurate analysis of the electromagnetic (EM) fields, it is very important to construct a "life-like" 3D model of the desired structure that includes both membrane supported structures and the surrounding thick dielectric substrate. This was not possible using analytical approaches or software packages based on Method-of-Moments, especially for frequencies up to W-band (75 - 110 GHz).

Refs. [10]-[12] describe the design of a complete 3D electromagnetic model for double folded slot antenna structures, processed through wet and dry micromachining of silicon. The electromagnetic simulations are validated by the experimental results up to 220 GHz.

This paper presents the first in depth 3D electromagnetic study, design, fabrication and characterization of a W-band membrane supported single folded slot antenna. The next section summarizes the main antenna parameters. Section 3 introduces the fully parametric 3D EM model developed for the analysis of the effect of both material and geometrical parameters. The optimized structure is then fabricated through DRIE of a high-resistivity (ρ > 5kOhm·cm) 525 µm thick silicon wafer (Section 4). A dedicated test setup is developed and the antenna test structure is characterized in terms of reflection losses and radiation properties. The measurement results are in good agreement with the simulations.

The antenna shows a measured fractional bandwidth of 36.43 % around 92.5 GHz and a simulated 3-dB gain bandwidth exceeding the W-band, making the proposed structure a good candidate for various applications, like passive/active imaging, high data-rate wireless communications, automotive radar applications etc.

2. Important antenna parameters

The antenna represents the interface between free-space and electronic circuits, enabling wireless communication by receiving/transmitting electromagnetic waves in a certain frequency range. This section shortly describes some of the main parameters which need to be taken into account when designing high-performance antennas [13].

One of the most important parameters is the *matching bandwidth*, which is usually defined for reflection losses lower than – 10 dB for an input impedance of 50 Ohm. This means that the electromagnetic energy that gets scattered back towards the input port is lower than – 10 dB. This delivered power is partly radiated and partly absorbed as losses in the antenna. A so-called *fractional bandwidth* can also be defined as the ratio between the bandwidth and the central operating frequency of the considered range.

The antenna *directivity* is a measure of the directionality of the antenna radiation characteristic and is calculated by dividing the power radiated per unit solid angle in a given direction by the total power radiated by the antenna.

The *gain* is a measure of the power radiated per unit solid angle in a given direction divided by the total input (or accepted) power from the source. This value is compared to the ideal isotropic radiator (radiates equally in all directions) and is usually expressed in dBi (or *decibels relative to isotropic*). It is the realized gain (which includes the mismatch losses and the internal ohmic losses of the antenna) which can be measured in practice. Another important performance indicator is the *3-dB gain bandwidth*, which is computed as the frequency range where the gain is higher than the maximum gain minus 3 dB. In other words, it is

the frequency range where the radiated power is still higher than half of the maximum radiated power in the given direction.

The *3D radiation characteristic* of the antenna shows the variation of the radiated power as a function of the radiation direction. If the 3D characteristic is cut by two orthogonal planes, *2D radiation characteristics* are obtained, as a function of the radiation angle. These are easier to plot, in either polar or rectangular form, and often chosen to coincide with the *E-plane* and, respectively, the *H-plane* of the antenna. On these 2D plots we can define a *main lobe* (containing the maximum radiation direction), a *half-power beam width* (or – *3 dB beam width*, which represents the angular range in which the radiated power decreases by half compared to the maximum) and the *sidelobes* (representing the inevitable radiation in unwanted directions).

An important parameter is the *radiation efficiency*, which describes the ratio of the power radiated by the antenna and the power accepted by the antenna, and includes the conduction and dielectric losses. Impedance mismatch losses are included in the *total efficiency* (which is always lower than the radiation efficiency).

3. EM analysis and design of the W-band folded slot antenna

3.1.EM modeling of membrane supported folded slot antennas

A fully parametric model of the membrane supported folded slot antenna was developed using the CST Microwave Studio 3D full-wave electromagnetic simulation software.

Unless otherwise stated, the electromagnetic models presented in this section are designed for a high-resistivity silicon substrate (>5kΩ·cm), with a thickness of 525 μm and a relative permittivity ε_{Si}=11.9. A two-layer membrane is considered. It consists of a 0.8 μm thick silicon dioxide layer (relative permittivity ε_{SiO2}=3.9) and a 0.6 μm thick silicon nitride layer (relative permittivity ε_{Si3N4}=8). These layers are modeled as a single, 1.4 μm thick layer with a relative permittivity ε_{eq}=4.9, computed according to (1) (equation adapted from [13]).

$$\frac{t_t}{\varepsilon_{eq}} = \sum_{i=1}^{N} \frac{t_i}{\varepsilon_i} \tag{1}$$

where: t_t is the total thickness of the dielectric layers; ε_{eq} is the equivalent relative permittivity; t_i is the thickness of the current layer; ε_i is the relative permittivity of the current layer; N is the total number of layers.

This equation is valid as long as the largest thickness is much smaller than the free space wavelength for the considered operating frequency.

The 3D view of the electromagnetic model developed for a membrane supported folded slot antenna is shown in Fig. 3.(a) The structure is surrounded by the silicon bulk with the vertical transition characteristic for the DRIE process.

Fig. 3.(b) shows the main geometrical parameters: w_3 is the width of the metallization inside the slot; l_3 is the length of the metallization; g_3 is the width of the slot surrounding the central metallization; (g3+d_slot) is the width of the upper slot; l_1 is length of the feeding CPW transmission line; w_1 is the width of the CPW signal line and g_1 is the width of the CPW slot.

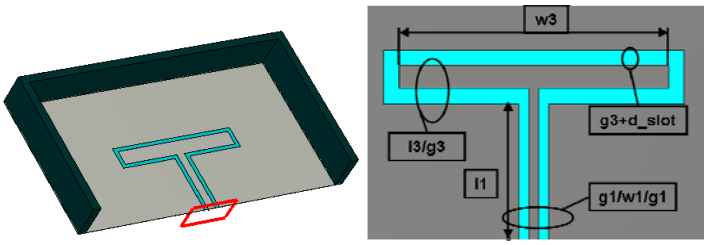

(a) (b)

Fig. 3. (a) 3D EM model of a membrane supported folded slot; (b) main geometrical parameters

According to [15], the impedance of a folded slot antenna can be estimated using Eq. (2) and (3)

$$Z_{slot} = \frac{Z_u}{4 \cdot Z_{dipol}} = \frac{377^2}{4 \cdot 70} \approx 500\Omega \tag{2}$$

$$Z_{IN} = \frac{Z_{slot}}{N^2} \tag{3}$$

where Z_u=377 Ω is the free space impedance, $Z_{dipol} \approx 70$ Ω is the impedance of a dipole operating in free space at its first resonance and N is the number of slots. Therefore, for a folded slot $Z_{IN} \approx 125$ Ω.

3.2. Design based on parametric studies

The parametric study of the folded slot antenna described in Fig. 3 begins with the analysis of the membrane supported feed CPW line impedance Z_{line}. The other parameters of the structure have the following values: w_3 = 1350 µm; l_3 = 120 µm; g_3 = 80 µm; d_slot =0; l_1= 1370 µm. The mean circumference of the slot (equal to $2 \cdot (w_3+l_3)+3/2 \cdot g_3+1/2 \cdot (g_3+d\_slot)$) = 3100 µm) is close to the free space wavelength at 94 GHz ($\lambda_{0,94GHz} \cong 3191$ µm). This is a basic rule of design for folded slot antennas [9].

Table 1 shows the characteristic membrane supported feed line impedances simulated with CST Microwave Studio, using a transient analysis, for different geometries of the CPW-TL, respectively different values for g_1 and w_1, as well as different values for the main fabrication parameters: the thickness of the membrane (t_{mem}) and the equivalent relative permittivity (ε_{mem}).

Table 1

Characteristic impedances for the membrane supported feed line

w_1 [µm]	g_1 [µm]	Z_{line} [Ω]	ε_{mem}	t_{mem} [µm]
50	25	113.739	4.9	1.4
50	50	145.142		
50	50	146.822		1
50	50	145.868	4.5	1.4
50	50	144.429	5.5	
50	75	168.237	4.9	
75	25	103.385		
75	50	133.066		
75	75	156.085		
100	25	84.6082		
100	50	125.263		
100	50	122.857	4.6	2
100	75	148.188	4.9	1.4
100	100	168.293		

It is demonstrated that a moderate variation (in the limit of the fabrication tolerances) of the technological parameters (t_{mem} and ε_{mem}) has only a slight influence on the input impedance. According to Table 1, a membrane supported CPW-TL with the signal line width w_1=100 µm and the gap g_1=50 µm, processed on a 1.4 µm thin dielectric membrane with a equivalent permittivity of 4.9, offers a line impedance of ~ 125 Ohm, therefore matching the antenna impedance. These values will be kept for further studies.

An example of a parametric study analyzing the effect of an asymmetric slot (the width of the upper slot – g_3+d_slot – is increased), is shown in Fig.4. An important effect on the minimum value of the |S11| parameter can be noticed (Fig.4.(a)), with a minor influence on the directivity (Fig.4.(b)). The optimum result is obtained for d_slot=0. It should be noted that the analyses made in this section consider the port impedance equal to the characteristic impedance of the membrane supported CPW-TL.

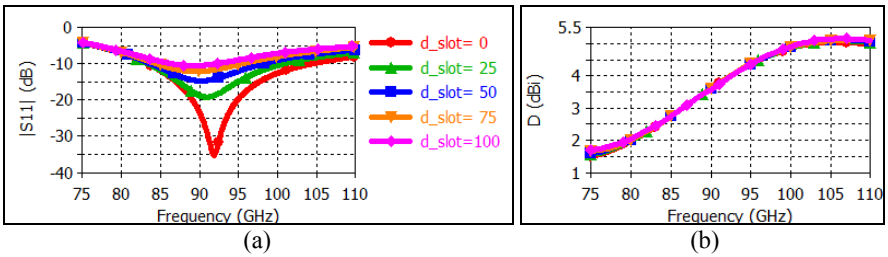

(a) (b)

Fig. 4. Simulated results for different values of the width of the slot: (a) reflection parameter; (b) directivity for the direction normal to the antenna plane

The structure was further optimized for wide operating bandwidth and a maximum radiation direction normal to the antenna surface for the 94 GHz frequency. Based on the technological results obtained for different dielectric layer combinations, a 1.95 μm thick dielectric membrane (consisting of 1.35 μm silicon oxide and 0.6 μm silicon nitride) was considered, released through deep reactive ion etching (DRIE) of a high resistivity silicon wafer. The following values were obtained for the geometrical parameters: w_3 = 1500 μm; l_3 = 200 μm; g_3 = 50 μm; d_slot =0; l_1= 800 μm; w_1 = 100 μm; g_1 = 50 μm.

The simulated |S11| parameter is shown in Fig. 5 (a). The operating bandwidth (defined for |S11| < – 10 dB) is between 82.5 – 110 GHz, with a minimum of – 23.8 dB at 93.4 GHz. Fig. 5 (b) shows the 3D gain characteristic at 94 GHz. The radiation characteristic shows two main lobes, almost symmetric with respect to the membrane. This is due to the structure being suspended on the thin membrane which causes it to behave as if it were suspended in air. This optimized characteristic has the maximum radiation direction normal to the antenna metallization. This is partly due to the matching of the feeding transmission line characteristic impedance to the input impedance of the antenna. The maximum gain is 5.58 dBi at 94 GHz. The analysis of the radiation characteristic in the whole W band shows maximum gains between 3.5 – 5.9 dBi, with little tilting of the maximum radiation direction and no sidelobes.

Fig. 5 (c) shows the electric field distribution at 94 GHz for the optimized antenna structure. The electric field distribution in the two slots is in phase, which determines an in phase adding of the radiated waves. This field distribution confirms the correct functioning of the structure. The electric field distribution along the membrane supported CPW feed is in good agreement with the basic propagation theory for this type of transmission line.

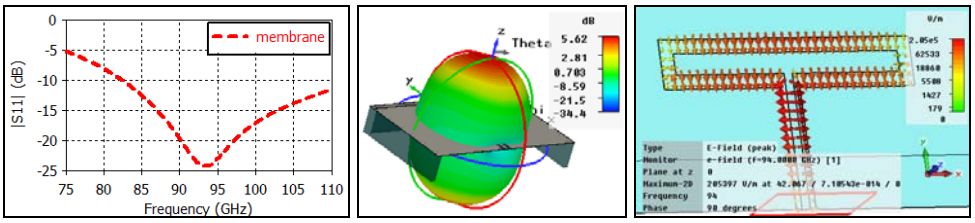

(a) (b) (c)

Fig. 5. Simulation results for the optimized antenna structure fed directly on the membrane: (a) |S11| parameter; (b) 3D gain characteristic at 94 GHz; (c) E field distribution at 94 GHz

3.3. Folded slot antenna with silicon bulk supported CPW-TL feed

Starting from the analysis presented in the previous sub-section, a bulk supported CPW-TL section was added for on-wafer characterization of the standalone antenna structure. This section consists of a quarter wavelength high-impedance CPW-TL (characteristic impedance of about 90 Ω, gap-signal-gap of

85-30-85 microns), followed by 50 Ω CPW-TL section, with the gap-signal-gap of 50-100-50 microns. The final layout is shown in Fig. 6.

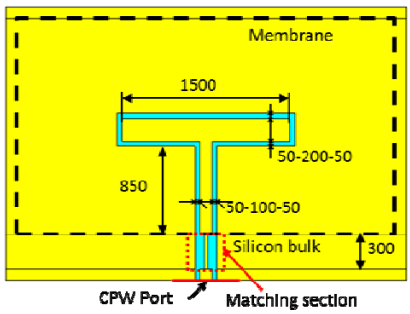

Fig. 6. Final layout of the membrane supported folded slot antenna

Fig. 7(a) shows a comparison between the simulated reflection parameter (|S11|) for the antenna excited directly on the membrane and the antenna excited from the silicon bulk area (according to the layout from Fig. 6). A slight frequency shift can be noticed. Fig. 7(b) shows the simulated gain as a function of frequency for the radiation direction normal to the antenna metallization for the antenna fed by the bulk supported CPW-TL. There is a gain of 4.3 – 5.1 dBi in the whole W band (75 – 110 GHz), which is a very good performance for a small size on-chip antenna.

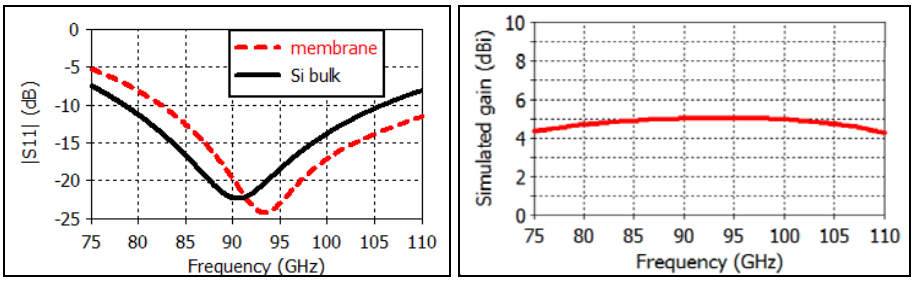

(a) (b)

Fig.7. (a) simulated |S11| for membrane excitation (dashed trace) and for silicon bulk excitation (solid trace); (b) simulated gain as a function of frequency for the radiation direction normal to the antenna plane for silicon bulk excitation

Fig. 8 shows the simulated 3D gain characteristic at 94 GHz. The radiation efficiency is higher than 85% at 94 GHz and higher than 80% in the whole W band. The total efficiency, which takes into account the mismatch losses of the antenna, is also very good over the whole W-band, with a peak value of 89% at 90 GHz and values better than 65 % in the whole W-band.

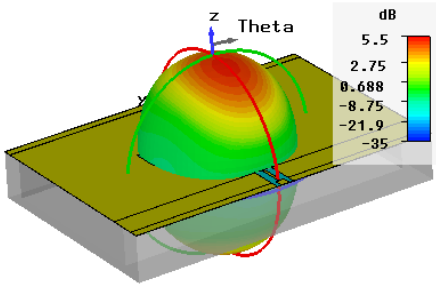

Fig.8. Simulated 3D radiation characteristic at 94 GHz

4. Fabrication and characterization results

The fabricated membrane consists of a 1.35 µm thick SiO_2 layer (grown through thermal oxidation) followed by a 0.6 µm thick Si_3N_4 (deposited through LPCVD – Low-Pressure Chemical Vapor Deposition) deposited on a high resistivity silicon wafer (ρ> 5 kOhm·cm) of 525 µm thickness. The membrane is released through deep reactive ion etching (DRIE) using the standard Bosh process in a ICP-RIE (Inductively Coupled Plasma – Reactive Ion Etching) PlasmaLab100 (Oxford Instruments) system [16].

The metallization consists of a 1 µm thick gold layer (obtained by sputtering, followed by electrochemical deposition) deposited on a 20 nm Cr adherence layer (obtained by sputtering).

Fig. 9(a) shows a detail of the frontside metallization of the fabricated structure. Fig. 9(b) shows a detail of the backside. The total size of the antenna is 3.6 x 2.45 mm^2 with a membrane area of 3.4 x 1.95 mm^2. Since the membrane is very thin, the slots in the frontside metallization are visible.

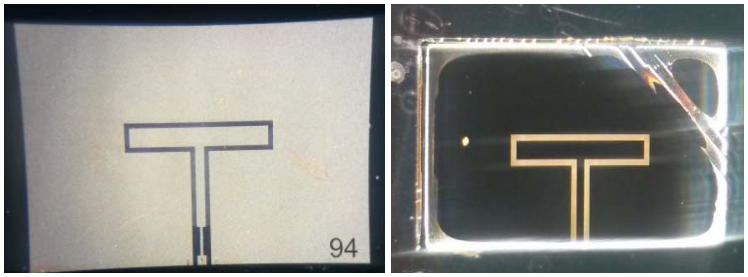

(a) (b)

Fig.9. Test structures: (a) detail of the frontside metallization; (b) detail of the backside

The folded slot antenna structures were measured on wafer using a Anritsu 37397D Vector Network Analyzer (VNA) with OML 65 – 110 GHz extension modules and a on wafer PM5 Suss Microtec characterization station. The station is dedicated for CPW measurements, using ground-signal-ground (G-S-G) probes

with a 150 µm pitch. The system was calibrated on wafer using a CS-5 standard calibration kit and the SOLT (short-open-load-thru) calibration procedure.

With this setup, the S11 parameter was recorded. A comparison between simulated and measured |S11| is shown in Fig. 10. A frequency shift of the measured minimum value can be noticed. This is mainly due to the imperfect processing (silicon residues around the membrane area), especially at the transition between the membrane and the silicon bulk for the antenna feed (see Fig. 9(b)). Even under these conditions it is very important to notice that the input matching bandwidth (|S11| < – 10 dB) is between 76.3 – 110 GHz, covering almost the whole W-band. The fractional bandwidth (calculated at 92.5 GHz) is of 36.43 %, while the minimum value of the measured |S11| is –29.72 dB at 82.37 GHz. For comparison, a silicon micromachined microstrip patch antenna has a bandwidth of about 5 % [17].

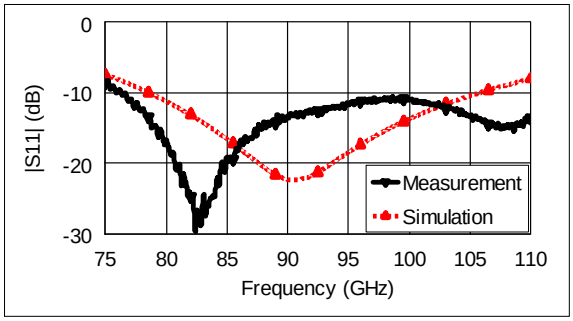

Fig.10. Comparison between measured (solid trace) and simulated (dashed) |S11| parameter

A photo of the antenna contacted on wafer is shown in Fig. 11(a). The second G-S-G probe can be noticed on the right side. This configuration was used to verify the radiation properties of the antenna. First, the second probe was placed above the antenna (close to the estimated maximum radiation direction), at a distance of about 3 cm (or 10 freespace wavelengths at 100 GHz). Then |S21| was recorded for two scenarios: 1. First probe above the antenna input, but not in contact; 2. First probe contacting the antenna input. The results of the two measurements are shown in Fig. 11(b). It can be noticed that the antenna radiates relatively uniform in the whole W band, in good agreement with the simulated gain (see Fig. 7(b)).

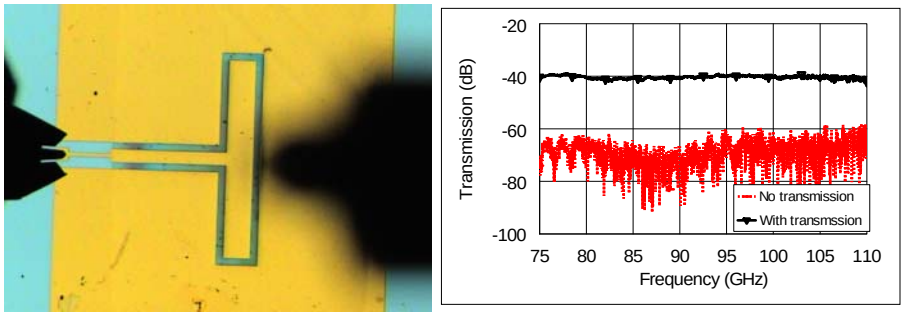

(a) (b)

Fig. 11. (a) membrane supported antenna during measurements; (b) comparison of the transmission parameter (|S21|) without (dotted trace) and with (solid trace) transmission

5. Conclusions

A membrane supported folded slot antenna for W-band applications was analyzed using 3D electromagnetic parametric simulations. A flexible 3D model was developed and the influence of material and geometrical parameters on input impedance, reflection losses and directivity for a membrane supported CPW-TL fed slot antenna were presented. First, the membrane fed structure was optimized for wide-band operation and good radiation performance, with the target of 94 GHz applications. Then, a transition to a bulk silicon CPW-TL was added and the structure was matched to 50 Ohm. A small profile (3.6 x 2.45 mm^2 for the whole chip), planar antenna was fabricated using deep reactive ion etching to release the 1.95 μm thin membrane. The measurement results show a matching bandwidth of 36.43 % with a simulated maximum gain of 5.16 dBi @ 92 GHz and a peak total efficiency of 89% at 90 GHz. The transmission measurements confirm a uniform radiation in the whole W-band. This antenna can be used as a standalone component and integrated either monolithically or hybrid in a W-band system for passive/active imaging, high data-rate wireless communications, automotive radar applications etc.

Acknowledgements

This work was supported by ROSA through the STAR project M3GAAS (CF 86/2013-2016), by the FP7 project NANOTEC (no. 288531) and by the project no. PN-II-ID-PCE-2011-3-0830.

REFERENCES

[1]. *H.M. Cheema, A. Shamim*, "The Last Barrier: On-Chip Antennas", IEEE Microw. Mag., vol. 14, no. 1, pp. 79–91, 2013.

[2]. *D.F.Filipovic; W.Y.Ali-Ahmad; G.M.Rebeiz,* "Millimeter-wave double-dipole antennas for high-gain integrated reflector illumination" IEEE Trans. on MTT, vol.40,no.5,pp.962-967, 1992

[3]. *G.M.Rebeiz*, RF MEMS -Theory, Design and Technology, New York: John Wiley & Sons, 2003
[4]. *C.Y.Chi, G.M.Rebeiz,*"Planar Microwave and Millimeter-Wave Lumped Elements and Coupled-Line Filters Using Micro-Machining Techniques", IEEE Trans. On MTT, vol.43, no.4, pp730-736, 1995
[5]. *D.Neculoiu, P.Pons, R.Plana, P.Blondy, A.Muller and D.Vasilache*, "MEMs antennas for millimeterwave applications", Proceeding of SPIE,vol.4559, pp.86-72, 2001
[6]. *D. Neculoiu; G. Bartolucci; G. Konstantinidis; R. Marcelli; I. Petrini; M. Dragoman; D. Vasilache; A. Muller*, "A micromachined 38 GHz Schottky-diode uniplanar monolithic integrated quasi-optical mixer," IEEE Radio Frequency Integrated Circuits (RFIC) Symposium, 2004. Digest of Papers., pp.531,534, 6-8 June 2004
[7]. *D. Neculoiu; I. Petrini; C. Buiculescu; M. Dragoman; A. Muller; G. Bartolucci; R. Marcelli; F. Giacomozzi*, "Design and characterization of a quasi-optical mixer fabricated using silicon micromachining" IEEE Mediterranean Electrotechnical Conference, pp.210-213, 2006
[8]. *A. Muller; D. Neculoiu; P. Pursula; T. Vaha-Heikkila; F. Giacomozzi; J. Tuovinen,* "Hybrid integrated micromachined receiver for 77 GHz millimeter wave identification systems," IEEE European Microwave Conference, pp.1034-1037, 9-12 Oct. 2007
[9]. *T.M. Weller; L.P.B. Katehi; G.M. Rebeiz,* "Single and double folded-slot antennas on semi-infinite substrates," IEEE Trans. on Ant. and Prop., vol.43, no.12, pp.1423-1428, 1995
[10]. *A.C.Bunea, D.Neculoiu, A.Muller*, "Analytic and Electromagnetic Investigation of Millimeter Wave Membrane Supported CPWs Processed on High Resistivity Silicon", Romanian J. Of Information Science And Technology, vol. 14, no.3, pp. 269–283, 2011
[11]. *A.C.Bunea, D.Neculoiu, P.Calmon, A.Takacs*: „Micromachined Front-End for 60 GHz Applications", IEEE Int. Semiconductor Conf., vol. 1, pp. 197-200, 2012
[12]. *A.-C. Bunea; A. Avram; C. Rusch; C. Obreja; D. Neculoiu*, „220 GHz Membrane Supported Folded Slot Antenna Array", IEEE International Semiconductor Conference, pp 93-96, 2013
[13]. *C.A. Balanis*, Antenna Theory – Analysis and Design; Chapter 2 – Fundamental Parameters of Antennas, pp. 27 – 132, 3rd ed., John Wiley & Sons, 2005
[14]. *W.K.W. Ali, S.H. Al-Charchafchi*: „Using equivalent dielectric constant to simplify the analysis of patch microstrip antenna with multi-layer substrates", IEEE International Symposium of Antennas and Propagation Society, 21-26 June 1998, vol.2, pp.676-679
[15]. *Huan-Shang Tsai; York, R.A.*, "FDTD analysis of CPW-fed folded-slot and multiple-slot antennas on thin substrates," IEEE Trans. on Ant. and Prop., vol.44, no.2, pp.217-226, 1996
[16]. *A. Avram, A.C. Bunea, C. Obreja, M. Avram, B. Bita, C. Parvulescu, M. Popescu, D. Neculoiu*, Fabrication of Thin Dielectric Membranes for RF-MEMS Applications, Digest Journal of Nanomaterials and Biostructures, Vol. 9, No. 2, pp. 475 – 481, 2014
[17]. *Papapolymerou, I.; Drayton, R.F.; Katehi, L.P.B.,* "Micromachined patch antennas," IEEE Trans. on Ant. and Prop., , vol.46, no.2, pp.275-283, 1998